

## Imaging the mechanics and electromechanics of the heart

Elisa E. Konofagou, *Associate Member, IEEE*, Simon Fung-kee-Fung,  
Jianwen Luo, *Member, IEEE*, and Mathieu Pernot

**Abstract**—The heart is a mechanical pump that is electrically driven. We have previously shown that the contractility of the cardiac muscle can reliably be used in order to assess the extent of ischemia using myocardial elastography. Myocardial elastography estimates displacement and strain during the natural contraction of the myocardium using signal processing techniques on echocardiograms in order to assess the change in mechanical properties as a result of disease. In this paper, we showed that elastographic techniques can be used to estimate and image both the mechanics and electromechanics of normal and pathological hearts in vivo. In order to image the mechanics throughout the entire cardiac cycle, the minimum frame rate was determined to be on the order of 150 fps in a long-axis view and 300 fps in a short-axis view. The incremental and cumulative displacement and strains were measured and imaged for the characterization of normal function and differentiation from infarcted myocardium. In order to image the electromechanical function, the incremental displacement was imaged in consecutive cardiac cycles during end-systole in both dogs and humans. The contraction wave velocity in normal dogs was found to be twice higher than in normal humans and twice lower than in ischemic dogs. In conclusion, we have demonstrated that elastographic techniques can be used to detect and quantify the mechanics and electromechanics of the myocardium in vivo. Ongoing investigations entail assessment of myocardial elastography in characterizing and quantifying ischemia and infarction in vivo.

### I. INTRODUCTION

Cardiovascular diseases rank as America's No. 1 killer, claiming the lives of over 41.4% of more than 2.4 million Americans who die each year. Cancer follows, killing 23%. All other causes of death account for about 35.3%. In addition, 61.8 million Americans have some form of cardiovascular disease. This includes diseases of the heart, stroke, high blood pressure, congestive heart failure, congenital heart defects, hardening of the arteries and other diseases of the circulatory system. Early detection of abnormality is thus the key in treating cardiovascular disease early and reducing the enormous death toll. The diagnosis of myocardial ischemia is often difficult to establish in its early stages when treatment is most effective. Patients suffering from myocardial ischemia may present to an emergency room or acute care facility with typical cardiac symptoms such as chest pain, described as tightness, pressure, or squeezing, but

Manuscript received April 24, 2006. This work was supported in part by the American Heart Association and the W.H Coulter Foundation. All authors are with the department of biomedical engineering of Columbia University, New York, NY 10027, USA (e-mail: ek2191@columbia.edu, M.Pernot is currently with Laboratoire Ondes et Acoustique, ESPCI, Paris, France.

some patients may have other symptoms such as arm or chin pain, nausea, sweating, or abdominal pain. Standard techniques such as the electrocardiogram (ECG) often provide inconclusive findings regarding ischemia, and sometimes may even be unable to identify situations, in which ischemia has progressed to cell damage and myocardial infarction (MI).

Elasticity imaging is a relatively new field that has dealt with the estimation and imaging of mechanically-related responses and properties for detection of pathological diseases, most notably cancer [1-3] and has thus emerged as an important field complementary to ultrasonic imaging. Only recently has the focus of the elasticity imaging field been steered towards cardiac applications [4-5]. This technique encompasses imaging of any kind of mechanical parameter that would highlight the mechanical property of the myocardium, such as displacement, strain, strain rate, velocity, shear strain, rotation angle, etc. In the same fashion as in standard elastography, the parameter that can relate directly to the underlying stiffness, and thereby to onset of disease, is the strain and the image that depicts the strain is called elastogram. Therefore, since assessment of the myocardial mechanical parameters has proven to be a crucial step in the detection of cardiac abnormalities, Myocardial Elastography can help make a significant impact in this field by measuring the mechanical response of the cardiac muscle at the various phases of the cardiac cycle [4]. Myocardial Elastography benefits from the development of techniques that can be used for high precision 2D time-shift based strain estimation techniques [6] and high frame rate currently available in ultrasound scanners [5] to obtain a detailed map of the transmural strain in normal [4-5] and pathological cases [7] over different phases and over several cardiac cycles. More recently, our group has shown that, by combining the two components of the strain tensors calculated from the two-dimensional displacements, the radial / circumferential / principal strains can be calculated as angle-independent measurements of the myocardial function [8].

In this paper, we identify the parameters under which myocardial elastography can be used in vivo to highlight the mechanics and electromechanics of the heart [9], in the absence or presence of disease.

### II. METHODS AND RESULTS

#### II.1. MECHANICS

##### II.1.1 Frame rate and correlation

In order to determine the frame rate that ensures the highest correlation and thereby most reliable strain estimates, the relationship between frame rate and correlation was

determined. The posterior wall of a normal human subject were imaged in short-axis and long-axis views, respectively, using a Vingmed Vivid FiVe (GE Vingmed, Horten, Norway) with a 2.5 MHz phased array. IQ (in-phase quadrature) data was acquired and transferred to a workstation for off-line analysis and converted back to RF. The sampling frequency was equal to 20 MHz and the depths and widths scanned ranged between 100-150 mm. In order to obtain axial (i.e., along the ultrasound beam) displacement and axial strain estimates, the cross-correlation method of consecutive RF segments was applied using a window equal to 2 mm and a window overlap of 80% to ensure high elastographic resolution [6]. The original frame rate was equal to 300 Hz and was progressively decimated to approximately 40 Hz in order to establish the relationship between correlation coefficients and frame rate (in frames/s or fps). The results from both long-axis and short-axis views are shown in Fig. 1.

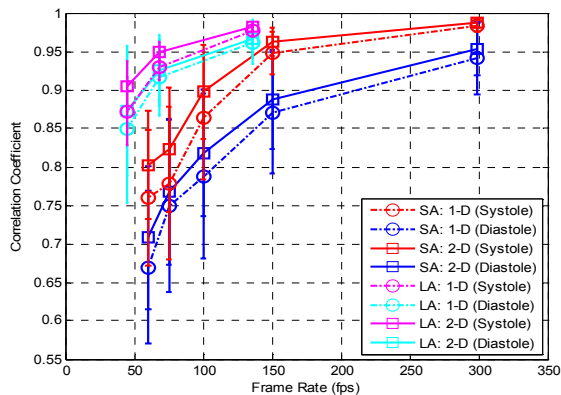


**Figure 1:** Correlation coefficient versus frame rate (fps) at different frame rate, from short axis view and long axis views, in systolic phase and diastolic phases, respectively. The errorbar indicates 0.5 standard deviation.

From Fig.1, there are several important observations that can be made. The correlation coefficient steadily increases with frame rate and slowly starts to reach a plateau beyond a certain frame rate. In the case of the long-axis view, that frame rate value is approximately 150 fps while in the case of the short-axis the value is twice higher, i.e., 300 fps. Also, during systole, the correlation coefficient is higher than during diastole. This is due to the fast filling phase that introduces high decorrelation as the strain rates are highest during that phase. Finally, 2D tracking, i.e., 1D kernel search in a 2D region, yields slightly higher correlations than 1D tracking. The crucial effect that frame rate can have on the strain imaged is shown in Fig. 2 in the most accentuated effect, i.e., during systole.

### II.1.2 Incremental displacements and strains

Using the same methods and parameters as in the previous section, incremental (i.e., frame-to-frame) strains were obtained in the posterior wall at 150 fps in a long-axis view.

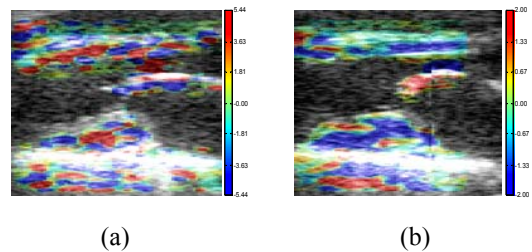


**Figure 2:** The importance of frame rate on strain accuracy: Compressive (blue) strains overlayed onto the long-axis echo view during diastole at a) 50 fps and b) 136 fps. Note how the quality of the image significantly increases at the higher frame rates.

Figure 3 shows the incremental displacement and strains obtained during systole and diastole.

### II.1.3 Cumulative displacements and strains

The cumulative (i.e., accumulating estimates over time starting at end-diastole) strains were obtained in the posterior wall at 300 fps in a short-axis view. The cumulative strains were obtained by summing over the incremental displacements (to obtain the cumulative displacements) and then performing the gradient operation on the cumulative displacements. The cumulative strain has been previously introduced as a higher quality alternative to incremental strain (Konofagou et al. 2003b) without any compromise on temporal resolution. Figure 4 shows the M-mode cumulative displacements and strains as well as correlation images obtained.

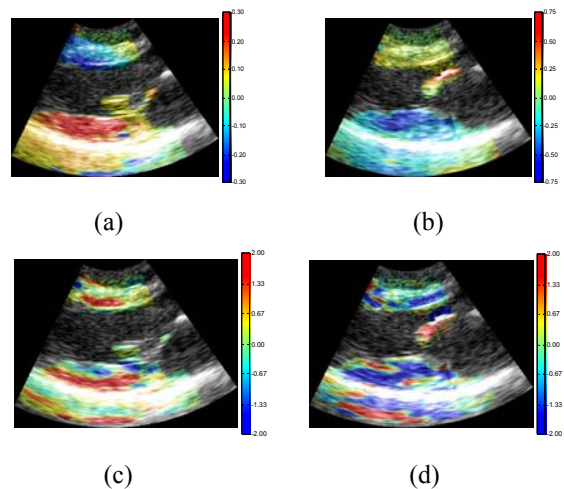


**Figure 3:** Incremental displacements in a long-axis views during a) systole and b) diastole and corresponding strains during c) systole and d) diastole. Blue and red displacements denote motion away from and towards the transducer (top on all images), respectively. Blue and red strains denote thickening and thinning, respectively.

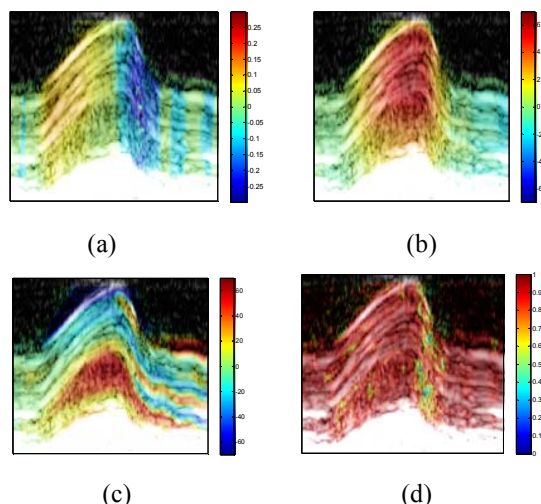


Figure 4: M-mode images - Variation over an entire cardiac cycle in a normal posterior wall: a) Incremental and b) cumulative displacements, c) cumulative strains and d) corresponding correlation coefficients.

#### II.1.4 Imaging for infarct detection

2D echocardiographic RF data using a portable, laptop scanner (Terason 2000, Teratech, Inc) and a 3 MHz phased array were acquired continuously during a 2-min induction of acute myocardial infarction through ligation of the left-ascending, distal (LAD) coronary artery of an open-chested dog (respiration was also interrupted). Sequences of ultrasound RF images were acquired at 54 fps (128 RF lines, sampling frequency: 10 MHz). Axial displacements are estimated from two consecutive RF frames, using a 1D cross-correlation algorithm (Size of the correlation windows: 6 mm; overlapping: 90%). In this algorithm, time-shifts between two consecutive backscattered signals are determined by the cross-correlation of small sliding windows over the entire 2D ultrasound image. Finally, the strain distribution is computed by differentiating the displacement map along the axial direction. For the numerical differentiation a least-squares regression method was used. The results show how elastograms and elastocardiograms (i.e., the overlaid echocardiogram and elastogram image, Fig.5) can be used to localize the region of the muscle undergoing ischemia (denoted by low strain (close to zero) between 3 o'clock and 6 o'clock, which coincides with the region of the LAD ligation).

## II.2. ELECTROMECHANICS

### II.2.1 Canine example in vivo

The experiments were performed in an anesthetized open-chested dog. The left descending artery (LAD) was ligated during surgery in order to induce ischemia. The ultrasound images were acquired using a commercial scanner (Terason 2000, Teratech, Inc.) with RF-data storage capability. The transducer was placed on the anterior wall of

the left ventricle of the heart, to obtain a short axis view. Approximately every two minutes, a sequence of three cardiac cycles was acquired during the experiment, with a frame rate of 56 fps. The motion detection technique was based on detecting the small displacements of the myocardium that occurs between two consecutive frames. Only axial displacements (in the direction of the transducer) were computed. The time-shifts in the backscattered signals are determined between the two consecutive frames through cross-correlation of small sliding windows (correlation windows of 3 mm, overlapping 90%) over the entire ultrasound image. This technique allows the detection of very small displacements on the order of 50  $\mu\text{m}$ .

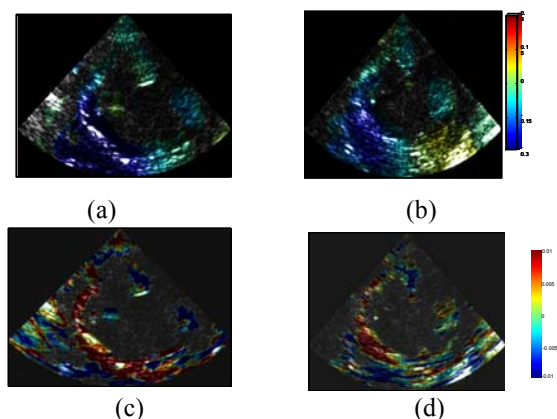


Figure 5: Canine ventricle *in vivo*: Displacement images (a-b) at end-diastole and corresponding elastocardiograms (c-d) at the beginning of and after 90 sec of LAD ligation, respectively. The strain ranges from +1% (compressive strain) to -1% (tensile strain). The ischemic region is shown increasing in size between 4 and 7 o'clock, close to the location of the LAD ligation.

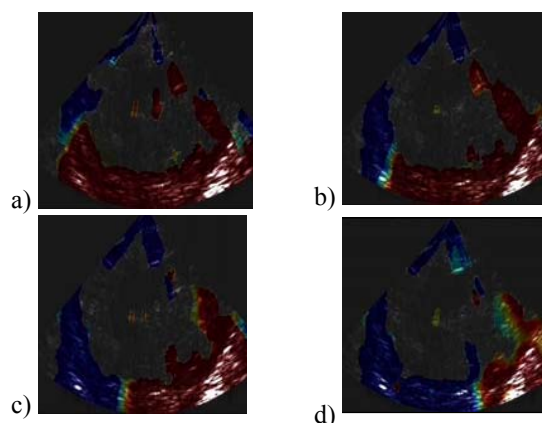
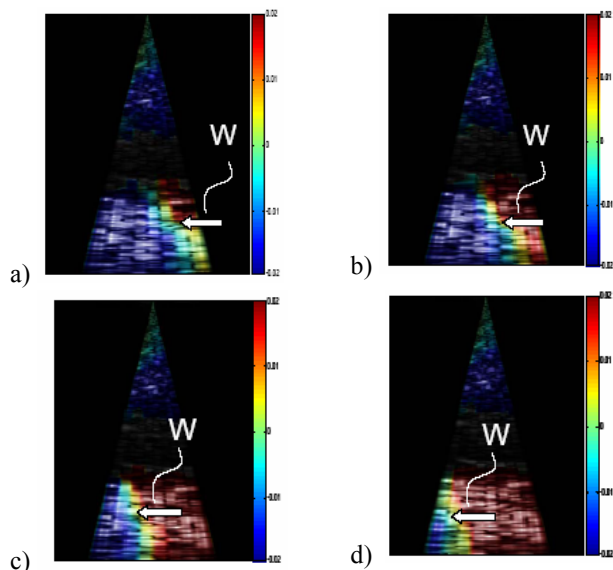


Figure 6: Canine example in vivo - Sequence showing the propagation of the contraction at a) 0 ms, b) 18 ms, c) 36 ms and d) 53 ms after end-systole. The displacements (in color) are overlaid onto the grayscale image. Blue and red displacements are towards and away from the transducer (located at top of the image), respectively. The frame rate is 56 images/s. The ischemic zone is located in the central bottom side of each image

On the cine-loop of the displacements, a strong contraction wave is clearly detected (Fig.1). The negative (blue) displacement indicating contraction of the myocardium propagates in the posterior wall from the septum (left side of the images) to the lateral wall (right side). The speed of the propagation was measured by tracking the contraction wavefront in the sequence. An average speed of 1.2m/s was found for the normal part of the heart, and 0.7 m/s for the ischemic region.



**Figure 7:** Human example in vivo - Sequence showing the propagation of the contraction at a) 6 ms, b) 18 ms, c) 30 ms and d) 36 ms after end-systole. The frame rate is 170 images/s. All the other parameters are the same as in Fig. 6.

### II.2.2 Human example in vivo

A sequence of approximately four cardiac cycles was acquired at a very high frame rate of 170 fps using a Vingmed System Five for RF image acquisition from a young, normal human subject. In order to reach such a high frame rate, only a small part of the heart (the left ventricle) was imaged (80 x 40 mm). The axial displacements were processed for each frame. On the displacement cine-loop, two electromechanical waves were clearly seen, propagating in the posterior wall of the left ventricular (not shown). Figure 7 shows consecutive displacement maps superimposed on the grayscale images in order to illustrate the propagation of the mechanical wave at the end-systolic phase. The speed was found to be 0.65 m/s in the posterior wall. The location of the electromechanical wavefront is indicated by arrow W in Figs. 7(a)-(d).

### III. CONCLUSION AND DISCUSSION

In this paper, we showed that elastographic techniques can be used to estimate and image both the mechanics and electromechanics of normal and pathological hearts in vivo. In order to image the mechanics throughout the entire cardiac cycle, the minimum frame rate to be used was on the order of

150 fps in a long-axis view and 300 fps in a short-axis view. The incremental and cumulative displacement and strains were measured and imaged for the characterization of normal function and differentiation from infarcted myocardium. In order to image the electromechanical function, the incremental displacement was imaged in consecutive cardiac cycles during end-systole in both dogs and humans. The contraction wave velocity in normal dogs was found to be twice higher than in normal humans and twice lower than in ischemic dogs. In conclusion, we have demonstrated that elastographic techniques can be used to detect and quantify the mechanics and electromechanics of the myocardium in vivo. Ongoing investigations entail assessment of myocardial elastography in characterizing and quantifying ischemia and infarction in vivo.

### IV. ACKNOWLEDGMENT

The authors wish to thank Kana Fujikura, M. D., for performing all the echocardiography scans used for this study.

### V. REFERENCES

- [1] K. J. Parker, S. R. Huang, R. A. Musulin and R. M. Lerner, Tissue response to mechanical vibrations for Sonoelasticity Imaging, *Ultrasound Med. Biol.*, 16, 241-246, 1990.
- [2] J. Ophir, I. Cespedes, H. Ponnekanti, Y. Yazdi, and X. Li, "Elastography: A quantitative method for imaging the elasticity of biological tissues," *Ultrason. Imaging*, vol. 13, pp. 111-134, 1991.
- [3] M.O'Donnell, A. R.Skovoroda, B. M. Shapo, and S. Y.Emelianov, Internal displacement and strain imaging using ultrasonic speckle tracking, *IEEE Trans. Ultrason. Ferroel. Freq. Cont.*, 41, 314-325, 1994.
- [4] E.E Konofagou., J. D'hooge and J.Ophir, Cardiac Elastography – A feasibility study, *IEEE Symposium in Ultrasonics, Ferroelectrics and Frequency Control*, San Juan, Puerto Rico, 1273-1276, 2000.
- [5] E. E. Konofagou, J. D'hooge, and J. Ophir, "Myocardial elastography - A feasibility study in vivo," *Ultrasound Med. Biol.*, vol. 28, pp. 475-482, 2002.
- [6] E.E. Konofagou and J Ophir., A New Elastographic Method for Estimation and Imaging of Lateral Strains, Corrected Axial Strains and Poisson's Ratios in Tissues, *Ultrasound in Medicine and Biology* 24(8), 1183-1199, 1998.
- [7] E. E. Konofagou, T. Harrigan, and S. Solomon, "Assessment of regional myocardial strain using cardiac elastography: Distinguishing infarcted from non-infarcted myocardium," *IEEE Ultrasonics Symp. Proc.*, 1589-1592, 2001.
- [8] S. D. Fung-Kee-Fung, W. N. Lee, C. M. Ingrassia, K. D. Costa, and E. E. Konofagou, "Angle-independent strain mapping in myocardial elastography 2D strain tensor characterization and principal component imaging," *IEEE Ultrasonics Symp. Proc.*, 516-519, 2005.
- [9] M. Pernot and E. E. Konofagou, "Electromechanical imaging of the myocardium at normal and pathological states," *IEEE Ultrasonics Symp. Proc.*, 1091-1094, 2005.